Quadruply Bonded Dimolybdenum Compounds with Polydentate Phosphines. 2. Structural and Spectroscopic Properties of *rac*-Mo$\overset{4}{-}$MoCl$_4$(PEt$_3$)(η^3-tetraphos-2) (tetraphos-2 = P(CH$_2$CH$_2$PPh$_2$)$_3$)

F. Albert Cotton* and Bo Hong

Department of Chemistry and The Laboratory for Molecular Structure and Bonding,
Texas A&M University, College Station, Texas 77843

Received December 16, 1992

The ligand substitution reaction between Mo$\overset{4}{-}$MoCl$_4$(PEt$_3$)$_4$ and the tetraphos-2 ligand, P(CH$_2$CH$_2$PPh$_2$)$_3$, yields the compound *rac*-Mo$\overset{4}{-}$MoCl$_4$(PEt$_3$)(η^3-tetraphos-2) that can be assigned as enantiomeric 1,2,5,7/1,2,6,8 type of isomer. This compound displays small torsional angles with an average of 11.7°. Thus the Mo$\overset{4}{-}$Mo bond distance (2.132(3) Å) is consequently shorter than those in the previously reported racemic (*R*,*R*, and *S*,*S*) and meso (*R*,*S* and *S*,*R*) Mo$_2$X$_4$(tetraphos-1) (tetraphos-1 = Ph$_2$PCH$_2$CH$_2$P(Ph)CH$_2$CH$_2$P(Ph)CH$_2$CH$_2$PPh$_2$, X = Cl, Br) compounds. The crystal structure of *rac*-Mo$\overset{4}{-}$MoCl$_4$(PEt$_3$)(η^3-tetraphos-2) is fully described. Crystallographic data for this compound are as follows: space group *Pna*2$_1$ with a = 16.979(3) Å, b = 16.061(3) Å, c = 21.280(7) Å, V = 5803(4) Å^3, and Z = 4. The ^{31}P{^{1}H} NMR spectrum of this complex displays five multiplets corresponding to five magnetically different phosphorus nuclei, and it affords a unique system to study ^{31}P–^{31}P coupling, through the connecting chain between phosphorus nuclei and/or through the metal–metal quadruple bond, in quadruply bonded dinuclear compounds. With use of the structural data for all the compounds with tetraphos-1 and tetraphos-2 ligands, the correlation between Mo$\overset{4}{-}$Mo bond distances and cos 2χ has been shown to be an inverse linear function with a correlation coefficient of 0.9672.

Introduction

Quadruply bonded dinuclear compounds of the M$_2$X$_4$L$_4$ type have already been much studied; references may be found in a monograph[1] as well as in the preceding paper[2] where we report the synthesis and characterization of the first examples of enantiomeric 1,2,5,8/1,2,6,7 and 1,2,5,7/1,2,6,8 type compounds, namely, Mo$_2$X$_4$(tetraphos-1) (tetraphos-1 = Ph$_2$PCH$_2$CH$_2$P(Ph)CH$_2$CH$_2$P(Ph)CH$_2$CH$_2$PPh$_2$, X = Cl, Br). Another frequently used tetraphosphine, the tripodal phosphine P(CH$_2$CH$_2$PPh$_2$)$_3$ (tetraphos-2), has been shown in the literature to function as tetradentate or, less commonly, tridentate ligand to one or two metal centers.[3] Much attention has been given to the studies of mononuclear systems with this ligand and their applications in homogeneous catalysis.[4] In most of these mononuclear compounds, the tetraphos-2 ligand spans four contiguous coordination sites on a trigonal bipyramid, a square pyramid, or an octahedron. Few dinuclear species with this ligand have been characterized. In [Au$_2$(μ-tetraphos-2)$_2$]Cl$_2$,[5] tetraphos-2 ligand acts in a different fashion involving both chelating and bridging, and each gold ion has a roughly tetrahedral geometry with three coordinated phosphorus atoms from one ligand and one phosphorus atom from another ligand molecule. The bridging arms of the tetraphos-2 ligand force the two gold atoms away from each other and give a nonbonding Au···Au distance of 6.199 Å. A similar coordination mode was postulated for the nickel complex Ni$_2$(μ-tetraphos-2)$_2$ on the basis of its ^{31}P{^{1}H} NMR spectrum.[6] We report here the synthesis, structure determination and spectroscopic study of the first case, namely, *rac*-Mo$\overset{4}{-}$MoCl$_4$(PEt$_3$)(η^3-tetraphos-2), where this ligand is employed in multiply bonded dinuclear systems. The central phosphorus atom of this achiral ligand becomes chiral on coordination due to the chelating/single-bridging coordination mode with one dangling –CH$_2$CH$_2$-PPh$_2$ unit.

Experimental Procedures

General Data. All manipulations were carried out under an atmosphere of argon unless otherwise specified. Standard Schlenk and vacuum line techniques were used. Commercial grade solvents were dried and deoxygenated by refluxing at least 24 h over the appropriate reagents and freshly distilled before use. Toluene, benzene, and *n*-hexane were purified by distillation from potassium/sodium benzophenone ketyl.

The tetraphos-2 ligand was purchased from Strem Chemicals and used as received (^{31}P{^{1}H} NMR data: −13.07 ppm (doublet), −17.39 ppm (quartet), $J_{\mathrm{P-P}}$ = 26 Hz). Mo$\overset{4}{-}$MoCl$_4$(PEt$_3$)$_4$ was prepared

---

(1) Cotton, F. A.; Walton, R. A. *Multiple Bond Between Metal Atoms*, 2nd ed.; Oxford University Press: London, 1993.

(2) Part 1: Chen, J.-D.; Cotton, F. A.; Hong, B. *Inorg. Chem.*, preceding paper in this issue.

(3) For a review on polydentate phosphines, see: Cotton, F. A.; Hong, B. *Progress in Inorganic Chemistry*; John Wiley: New York, 1992; Vol. 40, pp 179–189.

(4) (a) Gray, L. R.; Hale, A. L.; Levason, W.; McCullough, K. P.; Webster, M. *J. Chem. Soc., Dalton Trans.* **1984**, 47. (b) Antberg, M.; Dahlenberg, L. *Angew. Chem., Int. Ed. Engl.* **1986**, *25*, 260. (c) Bianchini, C.; Meli, A.; Peruzzini, M.; Vacca, A.; Zanobini, F. *Organometallics* **1987**, *6*, 2453. (d) Bianchini, C.; Mealli, C.; Peruzzini, M.; Zanobini, F. *J. Am. Chem. Soc.* **1987**, *109*, 5548. (e) Bianchini, C.; Peruzzini, M.; Vacca, A.; Zanobini, F. *J. Organomet. Chem.* **1987**, *326*, C79. (f) Bianchini, C.; Mealli, C.; Meli, A.; Peruzzini, M.; Zanobini, F. *J. Am. Chem. Soc.* **1988**, *110*, 8725. (g) Bianchini, C.; Peruzzini, M.; Zanobini, F. *J. Organomet. Chem.* **1988**, *354*, C19. (h) Bianchini, C.; Masi, D.; Meli, A.; Peruzzini, M.; Zanobini, F. *J. Am. Chem. Soc.* **1988**, *110*, 6411. (i) Gambaro, J. J.; Hohman, W. H.; Meek, D. W. *Inorg. Chem.* **1989**, *28*, 4154. (j) Bianchini, C.; Laschi, F.; Ottaviani, M. F.; Peruzzini, M.; Zanello, P.; Zanobini, F. *Organometallics* **1989**, *8*, 893. (k) Bianchini, C.; Laschi, F.; Peruzzini, M.; Ottaviani, F. M.; Vacca, A.; Zanello, P. *Inorg. Chem.* **1990**, *29*, 3394. (l) Bianchini, C.; Meli, A.; Peruzzini, M.; Zanobini, F.; Zanello, P. *Organometallics* **1990**, *9*, 241. (m) Bianchini, C.; Meli, A.; Peruzzini, M.; Zanobini, F.; Bruneau, C.; Dixneuf, P. H. *Organometallics* **1990**, *9*, 1155. (n) Bianchini, C.; Innocenti, P.; Meli, A.; Peruzzini, M.; Zanobini, F.; Zanello, P. *Organometallics* **1990**, *9*, 2514. (o) Bianchini, C.; Perez, P. J.; Peruzzini, M.; Zanobini, F.; Zanello, P. *Inorg. Chem.* **1991**, *30*, 279. (p) Bianchini, C.; Peruzzini, M.; Zanobini, F.; Frediani, P.; Albinati, A. *J. Am. Chem. Soc.* **1991**, *113*, 5453. (q) Bianchini, C.; Masi, D.; Linn, K.; Mealli, C.; Peruzzini, M.; Zanobini, F. *Inorg. Chem.* **1992**, *31*, 4036.

(5) Balch, A. L.; Fung, E. Y. *Inorg. Chem.* **1990**, *29*, 4764.

(6) Dubois, D. L.; Miedaner, A. *Inorg. Chem.* **1986**, *25*, 4642.

0020-1669/93/1332-2354$04.00/0

according to the published procedure.[7] The UV–vis data were collected on a Cary 17-D spectrophotometer. The $^{31}P\{^1H\}$ NMR and ^1H NMR spectra of *rac*-$Mo\overset{4}{-}MoCl_4(PEt_3)(\eta^3$-tetraphos-2) were recorded in CD_2Cl_2 solvent on Varian XL-200 and XL-400 spectrometers, respectively, with a total of 1600 or 16 transients. The $^{31}P\{^1H\}$ NMR chemical shift values were referenced externally and are reported relative to 85% H_3PO_4. Spectrum simulation was performed on a Sun Sparc 2 workstation using VnmrS Version 4.1 software. Chemical analyses were done by Galbraith Laboratories, Inc.

Preparation of *rac*-$Mo\overset{4}{-}MoCl_4(PEt_3)(\eta^3$-tetraphos-2). $Mo\overset{4}{-}MoCl_4(PEt_3)_4$ (0.15 g, 0.19 mmol) and tetraphos-2 ligand (0.13 g, 0.19 mmol) were suspended in 20 mL of toluene. This suspension was stirred and heated at reflux temperature for 3 h. Upon being heated, the suspended solids dissolved, and after approximately 30 min a green precipitate began to form. Stirring and heating were continued for an additional $2^1/_2$ h to ensure the completion of the reaction. The green precipitate was then filtered, washed with hexane, and dried in vacuo. Yield: 80%. Anal. Calcd for $Mo_2Cl_4P_5C_{48}H_{57}$: C, 51.35; H, 5.13. Found: C, 49.78; H, 5.06. UV–vis: 660 nm (3590 M^{-1} cm^{-1}), 452 nm (1040 M^{-1} cm^{-1}), 404 nm (1166 M^{-1} cm^{-1}), and 335 nm (6374 M^{-1} cm^{-1}).

Green prismatic crystals of this compound were obtained from the slow diffusion of hexane into a toluene/benzene (3:1) solution of the above product.

X-ray Crystallography

The crystal structure of *rac*-$Mo\overset{4}{-}MoCl_4(PEt_3)(\eta^3$-tetraphos-2)$\cdot C_6H_6$ was determined by a general procedure that has been fully described elsewhere.[8] Data reduction was carried out by standard methods with the use of well-established computational procedures.[9] The computations were done with Enraf-Nonius SDP software on a VAX computer.

A green prismatic crystal with dimensions of 0.15 × 0.10 × 0.10 mm was mounted on the top of a quartz fiber with epoxy cement. Crystal quality was verified by means of a rotation photograph. The unit cell was determined from the geometrical parameters of 25 well-centered reflections with 2θ values in the range 34.8–46.0°. The unit cell constants and axial photographs were consistent with an orthorhombic lattice, and the space group was shown to be *Pnma* or $Pna2_1$ by systematic absences. Refinement of the structure was successful in $Pna2_1$. The diffraction data were collected on a Rigaku AFC5R diffractometer at 20° by employing graphite monochromated Cu Kα radiation. Three standard reflections were measured periodically during the data collection to monitor any decay in intensity or change of crystal orientation. The intensities of all reflections with 2θ values in the range 4–115° were measured by the 2θ–ω scan technique. The structure factors were obtained after Lorentz and polarization corrections. Both decay and empirical absorption corrections were applied to the data. The latter were based on azimuthal (ψ) scans of reflections of Eulerian angle χ near 90°.[10]

The positions of the two molybdenum atoms and their coordinated atoms were found from a Patterson map. The positions of the remaining non-hydrogen atoms were located and refined by alternating difference Fourier syntheses and least-squares cycles. After the whole molecule has been refined to convergence, a difference Fourier map revealed six significant peaks which appeared to be a benzene molecule. This molecule was then refined with a rigid-body model in program SHELX-76[11] to convergence. The thermal parameter of the terminal atom C(5C2) in the PEt_3 unit was higher (31 Å^2) than the others, which indicated a possible disorder. However, from the difference Fourier map no separate peak could be found around this atom to determine a disorder model.

Pertinent crystallographic information is given in Table I, and Table II lists the positional and thermal parameters. Table III lists selected bond distances and angles. ORTEP diagrams of the whole molecule and of its projection along $Mo\overset{4}{-}Mo$ axis are given in Figures 1 and 2, respectively, while tables of anisotropic thermal parameters, complete bond lengths and angles, and complete torsional angles along the $Mo\overset{4}{-}Mo$ bond are available as supplementary material.

Table I. Crystallographic Data and Data Collection Parameters for *rac*-$Mo\overset{4}{-}MoCl_4(PEt_3)(\eta^3$-tetraphos-2)$\cdot C_6H_6$

chem formula	$Mo_2Cl_4P_5C_{54}H_{63}$	V, Å^3	5803(4)
fw	1200.67	Z	4
space group	$Pna2_1$	T, °C	20 ± 1
a, Å	16.979(3)	λ, Å	1.541 84
b, Å	16.061(3)	ρ_{calcd}, g cm^{-3}	1.374
c, Å	21.280(7)	μ(Cu Kα), cm^{-1}	69.34
α, deg	(90)	data colln instrum	Rigaku AFC5R
β, deg	(90)	transm coeff	1.000–0.950
γ, deg	(90)	R,[a] R_w[b]	0.0640, 0.0787

[a] $R = \sum||F_o| - |F_c|| / \sum|F_o|$. [b] $R_w = [\sum w(|F_o| - |F_c|)^2 / \sum w|F_o|^2]^{1/2}$; $w = 1/\sigma^2(|F_o|)$.

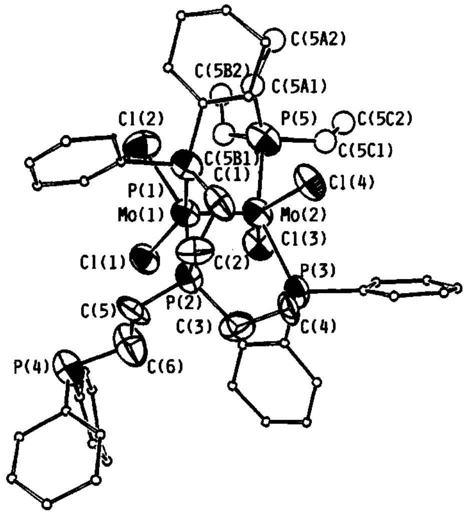

Figure 1. ORTEP drawing of the $Mo\overset{4}{-}MoCl_4(PEt_3)(\eta^3$-tetraphos-2) molecule. Thermal ellipsoids are drawn at the 50% probability level. For clarity, all of the carbon atoms except those on the ethylene connecting chains between phosphorus atoms are drawn as circles of arbitrary size.

Results and Discussion

Synthesis and Structure. The ligand substitution reaction between $Mo\overset{4}{-}MoCl_4(PEt_3)_4$ and 1 molar equiv of tetraphos-2 ligand in toluene gives the green product *rac*-$Mo\overset{4}{-}MoCl_4(PEt_3)(\eta^3$-tetraphos-2) in 80% yield. The purity of this compound is verified by the $^{31}P\{^1H\}$ NMR, ^1H NMR, UV–vis spectra and analysis of the product. Green prismatic crystals were obtained by slow diffusion of hexane into a toluene/benzene (3:1) solution of this compound.

Crystals of *rac*-$Mo\overset{4}{-}MoCl_4(PEt_3)(\eta^3$-tetraphos-2) conform to the space group $Pna2_1$ with four molecules per unit cell. Figure 1 depicts the structure of one molecule in its entirety. The ligand tetraphos-2 adopts a chelating/single-bridging mode with one dangling $-CH_2CH_2PPh_2$ unit. Thus the central phosphorus atom of this achiral ligand becomes chiral on coordination. Since two molecules in each unit cell of the achiral space group $Pna2_1$ have the *R* chirality and the other two possess the *S* chirality, we have obtained a racemic (*R* and *S*) diastereomer. The $Mo\overset{4}{-}Mo$ bond distance is 2.132(3) Å, which falls within the range of the distances established for the Mo–Mo quadruple bond. Compared with the $Mo\overset{4}{-}Mo$ bond distances in racemic (*R,R* and *S,S*) and meso (*R,S* and *S,R*) Mo_2X_4(tetraphos-1), 2.154 and 2.190 Å, respectively,[2] this bond distance is significantly shorter.

Although in some cases $Mo_2X_4P_4$ compounds are found to conform closely to the ideal of square parallelepipeds with a

---

(7) (a) Cotton, F. A.; Daniels, L. M.; Powell, G. L.; Kahaian, A. J.; Smith, T. J.; Vogel, E. F. *Inorg. Chim. Acta* **1988**, *144*, 109. (b) Glicksman, H. D.; Hamer, A. D.; Smith, T. J.; Walton, R. A. *Inorg. Chem.* **1976**, *15*, 2205.

(8) (a) Bino, A.; Cotton, F. A.; Fanwick, P. E. *Inorg. Chem.* **1979**, *18*, 3558. (b) Cotton, F. A.; Frenz, B. A.; Deganello, G.; Shaver, A. J. *J. Organomet. Chem.* **1979**, *50*, 227.

(9) Crystallographic computing was done on a local area VAX cluster employing the VAX/VMS V5.4 computer.

(10) North, A. C. T.; Phillips, D. C.; Mathews, F. S. *Acta Crystallogr., Sect. A*, **1968**, *24*, 351.

(11) Sheldrick, G. M. SHELX-76, a system of computer programs for X-Ray Structure Determination. University of Cambridge, Cambridge, England, 1976.

Table II. Positional and Thermal Parameters for Non-Hydrogen Atoms of *rac*-$\mathrm{Mo}\overset{4}{-}\mathrm{MoCl_4(PEt_3)}(\eta^3\text{-tetraphos-2})\cdot\mathrm{C_6H_6}$

atom	*x*	*y*	*z*	B_{eq},[a] Å^2
Mo(1)	0.23881(9)	0.1730(1)	0.000	4.40(4)
Mo(2)	0.2616(1)	0.1277(1)	0.0924(1)	4.89(4)
Cl(1)	0.1493(3)	0.2861(3)	0.0103(3)	5.3(1)
Cl(2)	0.1240(4)	0.1017(4)	–0.0490(4)	6.9(2)
Cl(3)	0.1654(3)	0.1900(4)	0.1620(3)	5.7(1)
Cl(4)	0.3751(3)	0.0348(3)	0.0917(3)	6.2(1)
P(1)	0.3281(4)	0.0855(4)	–0.0682(3)	5.1(2)
P(2)	0.3681(3)	0.2575(4)	–0.0194(3)	4.7(1)
P(3)	0.3705(3)	0.2199(3)	0.1422(3)	4.8(1)
P(4)	0.2734(5)	0.4874(5)	–0.0903(4)	8.1(2)
P(5)	0.1637(4)	0.0100(4)	0.1043(4)	7.0(2)
C(1)	0.440(1)	0.113(1)	–0.055(1)	5.3(6)
C(2)	0.447(1)	0.200(1)	–0.065(1)	4.7(5)
C(3)	0.436(1)	0.299(2)	0.043(1)	6.0(6)
C(4)	0.462(1)	0.238(1)	0.091(1)	4.9(5)
C(5)	0.353(1)	0.343(1)	–0.070(1)	6.1(7)
C(6)	0.313(2)	0.409(2)	–0.036(1)	8.8(9)
C(1A1)	0.314(1)	0.118(2)	–0.152(1)	6.1(7)
C(1B1)	0.320(1)	–0.021(1)	–0.077(1)	5.8(6)
C(3A1)	0.341(1)	0.317(1)	0.171(1)	5.0(5)
C(3B1)	0.418(1)	0.172(1)	0.213(1)	5.3(6)
C(4A1)	0.215(3)	0.544(2)	–0.031(2)	11(1)
C(4B1)	0.360(2)	0.539(2)	–0.109(1)	8.8(9)
C(5A1)	0.184(2)	–0.072(2)	0.047(2)	12(1)
C(5B1)	0.050(1)	0.037(2)	0.097(2)	10(1)
C(5C1)	0.187(3)	–0.027(2)	0.188(3)	16(2)
C(1A2)	0.368(1)	0.079(1)	–0.199(1)	6.0(5)*
C(1A3)	0.365(2)	0.112(2)	–0.257(1)	7.9(7)*
C(1A4)	0.318(2)	0.171(2)	–0.273(2)	9.0(8)*
C(1A5)	0.265(1)	0.209(2)	–0.230(1)	6.9(6)*
C(1A6)	0.261(2)	0.177(2)	–0.168(1)	7.1(6)*
C(1B2)	0.380(2)	–0.064(2)	–0.047(1)	7.9(7)*
C(1B3)	0.376(2)	–0.156(2)	–0.053(2)	10.2(9)*
C(1B4)	0.303(2)	–0.178(2)	–0.089(2)	10.8(9)*
C(1B5)	0.245(2)	–0.139(2)	–0.122(2)	8.6(7)*
C(1B6)	0.255(2)	–0.051(2)	–0.115(2)	8.3(7)*
C(3A2)	0.275(1)	0.355(1)	0.145(1)	5.9(5)*
C(3A3)	0.259(2)	0.435(2)	0.164(2)	9.3(8)*
C(3A4)	0.308(2)	0.468(2)	0.212(1)	8.0(7)*
C(3A5)	0.377(2)	0.432(2)	0.236(1)	8.9(8)*
C(3A6)	0.396(2)	0.355(2)	0.215(1)	7.6(7)*
C(3B2)	0.501(1)	0.153(2)	0.215(1)	6.4(6)*
C(3B3)	0.526(2)	0.116(2)	0.271(1)	8.3(7)*
C(3B4)	0.476(2)	0.108(2)	0.318(1)	8.6(7)*
C(3B5)	0.393(2)	0.122(2)	0.317(2)	11(1)*
C(3B6)	0.359(2)	0.160(2)	0.260(2)	9.0(8)*
C(4A2)	0.259(2)	0.606(3)	–0.006(2)	11(1)*
C(4A3)	0.218(3)	0.640(4)	0.045(3)	18(2)*
C(4A4)	0.130(3)	0.625(2)	0.060(2)	12(1)*
C(4A5)	0.095(2)	0.554(3)	0.037(2)	11(1)*
C(4A6)	0.144(2)	0.515(2)	–0.007(2)	10.7(9)*
C(4B2)	0.350(2)	0.607(2)	–0.153(2)	8.7(8)*
C(4B3)	0.413(2)	0.660(2)	–0.168(2)	9.0(8)*
C(4B4)	0.488(2)	0.665(2)	–0.141(2)	9.9(8)*
C(4B5)	0.506(3)	0.599(3)	–0.098(2)	14(1)*
C(4B6)	0.438(2)	0.542(2)	–0.085(2)	11(1)*
C(5A2)	0.157(3)	–0.158(3)	0.062(3)	17(2)*
C(5B2)	–0.015(2)	–0.024(2)	0.099(2)	11.3(9)*
C(5C2)	0.157(6)	–0.069(6)	0.219(6)	31(5)*
C(7)	0.549(2)	0.250(2)	0.705(2)	15.5(6)*
C(8)	0.565(2)	0.169(2)	0.685(2)	15.5(6)*
C(9)	0.587(2)	0.108(2)	0.729(2)	15.5(6)*
C(10)	0.592(2)	0.129(2)	0.792(2)	15.5(6)*
C(11)	0.576(2)	0.210(2)	0.812(2)	15.5(6)*
C(12)	0.554(2)	0.270(2)	0.769(2)	15.5(6)*

[a] Values for anisotropically refined atoms are given in the form of the equivalent isotropic displacement parameter defined as $^1/_3[a^2a^{*2}B_{11} + b^2b^{*2}B_{22} + c^2c^{*2}B_{33} + 2ab(\cos\gamma)a^*b^*B_{12} + 2ac(\cos\beta)a^*c^*B_{13} + 2bc(\cos\alpha)b^*c^*B_{23}]$. Starred values denote atoms that were refined isotropically.

Table III. Selected Bond Lengths (Å) and Angles (deg) for *rac*-$\mathrm{Mo}\overset{4}{-}\mathrm{MoCl_4(PEt_3)}(\eta^3\text{-tetraphos-2})\cdot\mathrm{C_6H_6}$

Mo(1)–Mo(2)	2.132(3)	Mo(2)–P(5)	2.529(7)
Mo(1)–Cl(1)	2.378(5)	P(1)–C(1)	1.98(2)
Mo(1)–Cl(2)	2.490(7)	P(2)–C(2)	1.89(2)
Mo(1)–P(1)	2.526(6)	P(2)–C(3)	1.88(2)
Mo(1)–P(2)	2.613(6)	P(3)–C(4)	1.91(2)
Mo(2)–Cl(3)	2.422(6)	P(2)–C(5)	1.77(2)
Mo(2)–Cl(4)	2.437(6)	P(4)–C(6)	1.83(3)
Mo(2)–P(3)	2.595(6)		

Mo(2)–Mo(1)–Cl(1)	107.0(2)	Mo(1)–Mo(2)–P(3)	108.1(2)
Mo(2)–Mo(1)–Cl(2)	111.8(2)	Mo(1)–Mo(2)–P(5)	103.2(2)
Mo(2)–Mo(1)–P(1)	103.4(2)	Cl(3)–Mo(2)–Cl(4)	142.2(3)
Mo(2)–Mo(1)–P(2)	99.8(1)	Cl(3)–Mo(2)–P(3)	89.7(2)
Cl(1)–Mo(1)–Cl(2)	83.6(2)	Cl(3)–Mo(2)–P(5)	78.7(2)
Cl(1)–Mo(1)–P(1)	149.4(2)	Cl(4)–Mo(2)–P(3)	77.8(2)
Cl(1)–Mo(1)–P(2)	98.9(2)	Cl(4)–Mo(2)–P(5)	93.6(2)
Cl(2)–Mo(1)–P(1)	88.5(2)	P(3)–Mo(2)–P(5)	148.6(3)
Cl(2)–Mo(1)–P(2)	146.1(2)	Mo(1)–P(1)–C(1)	111.7(7)
P(1)–Mo(1)–P(2)	72.2(2)	Mo(1)–P(2)–C(2)	115.0(6)
Mo(1)–Mo(2)–Cl(3)	107.5(2)	Mo(1)–P(2)–C(3)	126.1(7)
Mo(1)–Mo(2)–Cl(4)	110.3(2)	Mo(2)–P(3)–C(4)	115.6(7)
Mo(1)–P(2)–C(5)	112.3(8)		

[a] Numbers in parenthesis are estimated standard deviations in the least significant digit.

torsional angle χ of 0°, most of the compounds of this type tend to adopt twisted configurations with torsional angles ranging from 0 to 90°. The projection of the inner part of the molecule of *rac*-$\mathrm{Mo}\overset{4}{-}\mathrm{MoCl_4(PEt_3)}(\eta^3\text{-tetraphos-2})$ along the Mo–Mo axis, shown in Figure 2a, displays such a distortion. The internal rotational angle P(2)–Mo(1)–Mo(2)–P(3) is 19.4°, while the other three angles Cl(1)–Mo(1)–Mo(2)–Cl(3), Cl(2)–Mo(1)–Mo(2)–P(5), and P(1)–Mo(1)–Mo(2)–Cl(4) are 12.5, 4.7, and 10.0°, respectively. Thus the average torsional angle χ is 11.7°. A small nonbonded steric repulsion in this molecule, resulting from the presence of the dangling $-\mathrm{CH_2CH_2PPh_2}$ unit and a chelating/single-bridging coordination mode of the tetraphos-2 ligand, may account for the small torsional angles in this compound. This racemic compound comprises the 1,2,5,7/1,2,6,8 type of isomer, as shown in the "cubic" drawing of the central part in Figure 2b.

The $\mathrm{Mo}\overset{4}{-}\mathrm{Mo}$ bond distances and torsional angles for a series of quadruply bonded dimolybdenum compounds with tetradentate phosphine ligands are compared in Table IV. A study on the correlation between the $\mathrm{Mo}\overset{4}{-}\mathrm{Mo}$ bond distance and cos 2χ has been done. A least-squares line, as shown in Figure 3, can be drawn with a correlation coefficient of –0.9627. Since the δ-overlap is also proportional to cos 2χ,[12] this result indicates that the bond length is in linear proportion to decreasing δ-bond strength. A similar result was also obtained previously in the correlation study on a series of quadruply bonded dimolybdenum compounds with bidentate phosphine ligands.[13,14] Since a perfect linear relationship will have a correlation coefficient of +1 or –1, this correlation coefficient of –0.9627 indicates that, as expected, other factors such as steric repulsion and coordination mode, etc., also play a role in determining the bond length.

Spectroscopic Properties. UV–Vis Spectroscopy. Figure 4 shows the absorption spectrum of *rac*-$\mathrm{Mo}\overset{4}{-}\mathrm{MoCl_4(PEt_3)}$ (η^3-tetraphos-2) in $\mathrm{CH_2Cl_2}$. It displays four distinct bands. The lowest energy band at 660 nm (15 152 cm^{-1}) with an absorption coefficient of 3590 M^{-1} cm^{-1} is assigned to the $\delta_{xy} \rightarrow \delta^*_{xy}$

---

(12) Cotton, F. A.; Fanwick, P. E.; Fitch, J. W.; Glicksman, H. D.; Walton, R. A. *J. Am. Chem. Soc.* **1979**, *101*, 1752.

(13) Campbell, F. L., III; Cotton, F. A.; Powell, G. L. *Inorg. Chem.* **1985**, *24*, 4384.

(14) Campbell, F. L., III; Cotton, F. A.; Powell, G. L. *Inorg. Chem.* **1984**, *23*, 4222.

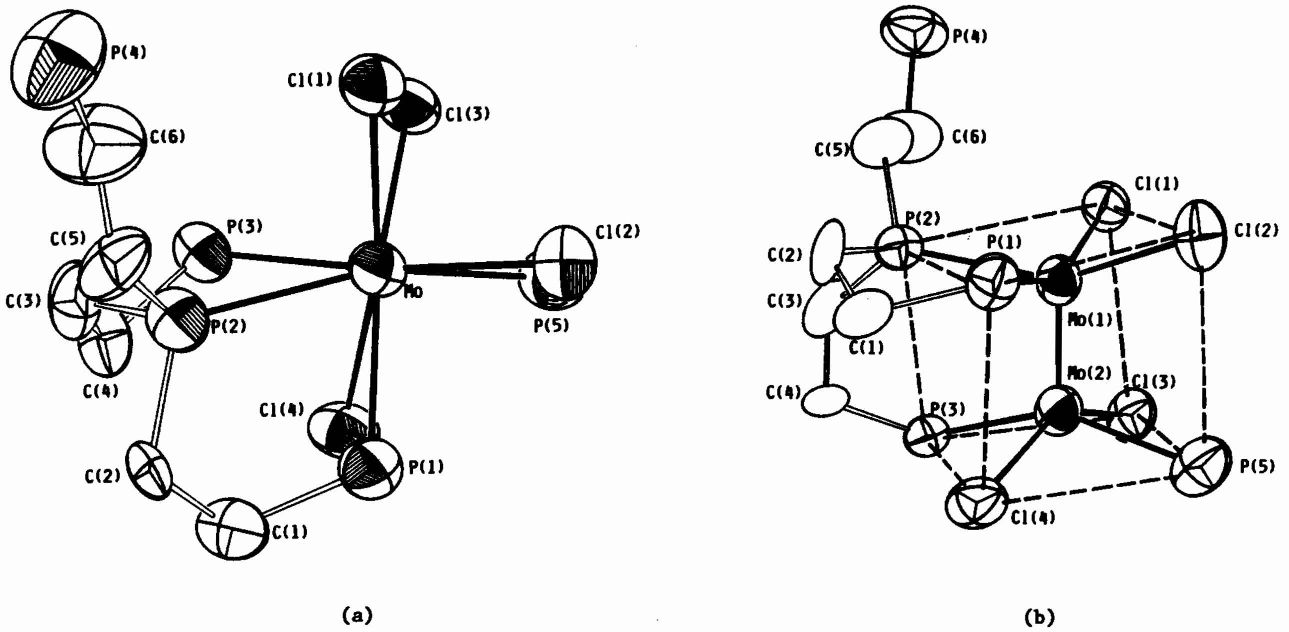

Figure 2. (a) Projection of the inner part along the $\mathrm{Mo}\overset{4}{-}\mathrm{Mo}$ axis in *rac*-$\mathrm{Mo}\overset{4}{-}\mathrm{MoCl_4(PEt_3)}(\eta^3$-tetraphos-2)·$C_6H_6$. (b) Skeletal drawing of the inner part of *rac*-$\mathrm{Mo}\overset{4}{-}\mathrm{MoCl_4(PEt_3)}(\eta^3$-tetraphos-2)·$C_6H_6$. (All thermal ellipsoids are drawn at 50% probability).

Table IV. Comparison of the $\mathrm{Mo}\overset{4}{-}\mathrm{Mo}$ Bond Distances and Torsional Angles for $M_2X_4P_4$ Compounds with Tetraphosphines

complexes	Mo–Mo, Å	χ,[a] deg	isomer type
rac-$\mathrm{Mo}\overset{4}{-}\mathrm{MoCl_4}$(tetraphos-1)·$CH_2Cl_2$[b,c]	2.1549(4)	18.5	1,2,6,7/1,2,5,8
meso-$\mathrm{Mo}\overset{4}{-}\mathrm{MoCl_4}$(tetraphos-1)[c]	2.186(1)	30.9(1)	1,2,5,7/1,2,6,8
rac-$\mathrm{Mo}\overset{4}{-}\mathrm{MoBr_4}$(tetraphos-1)·0.5$CH_2Cl_2$[c]	2.1520(6)	19.13(5)	1,2,6,7/1,2,5,8
meso-$\mathrm{Mo}\overset{4}{-}\mathrm{MoBr_4}$(tetraphos-1)·$CH_2Cl_2$[c]	2.189(3)[d]	30.7(3)	1,2,5,7/1,2,6,8
meso-$\mathrm{Mo}\overset{4}{-}\mathrm{MoBr_4}$(tetraphos-1)·1.5THF[c]	2.195(1)	28.6(1)	1,2,5,7/1,2,6,8
rac-$\mathrm{Mo}\overset{4}{-}\mathrm{MoCl_4(PEt_3)}(\eta^3$-tetraphos-2)·$C_6H_6$[e]	2.132(3)	11.7(3)	1,2,5,7/1,2,6,8

[a] Average torsional angle. [b] See ref 19. [c] See ref 2. [d] Average data for molecule A and B. [e] This work.

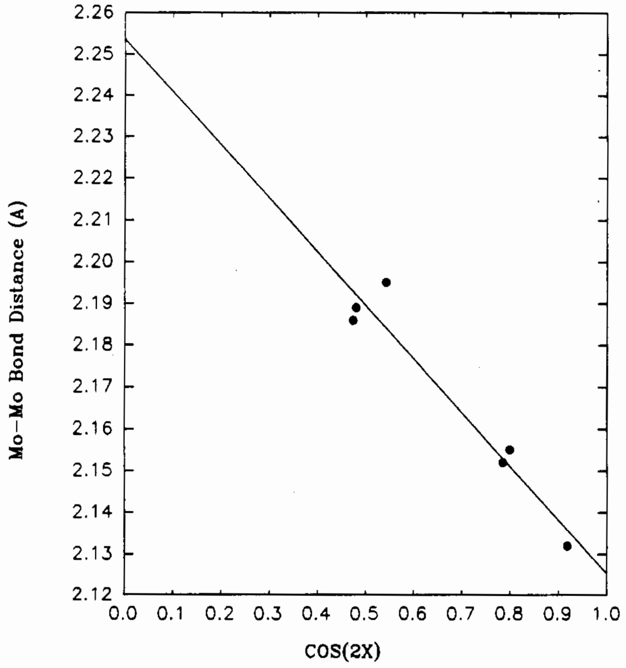

Figure 3. Plot of $\mathrm{Mo}\overset{4}{-}\mathrm{Mo}$ bond distances vs cos 2χ.

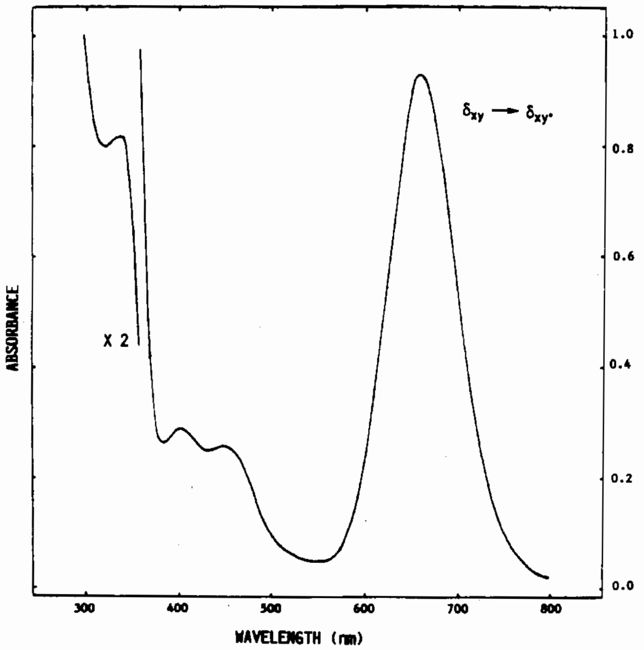

Figure 4. Electronic absorption spectrum of *rac*-$\mathrm{Mo}\overset{4}{-}\mathrm{MoCl_4(PEt_3)}$ (η^3-tetraphos-2) in CH_2Cl_2 (concentration used, 2.602 × 10^{-4} M; cell path; 1 cm).

transition.[1,15] Compared with the corresponding bands (the absorption coefficients are in the range 200–700 M^{-1} cm^{-1}) of the quadruply bonded dimolybdenum compounds with tetraphos-1 ligands, this band has a much higher intensity. As is well-known,[1] this higher intensity is the result of better overlap between the d_{xy} orbitals due to the small torsional angle in this compound,

---

(15) Agaskar, P. A.; Cotton, F. A.; Fraser, I. F.; Manojlovic-Muir, L.; Muir, K. W.; Peacock, R. D. *Inorg. Chem.* **1986**, *25*, 2511.

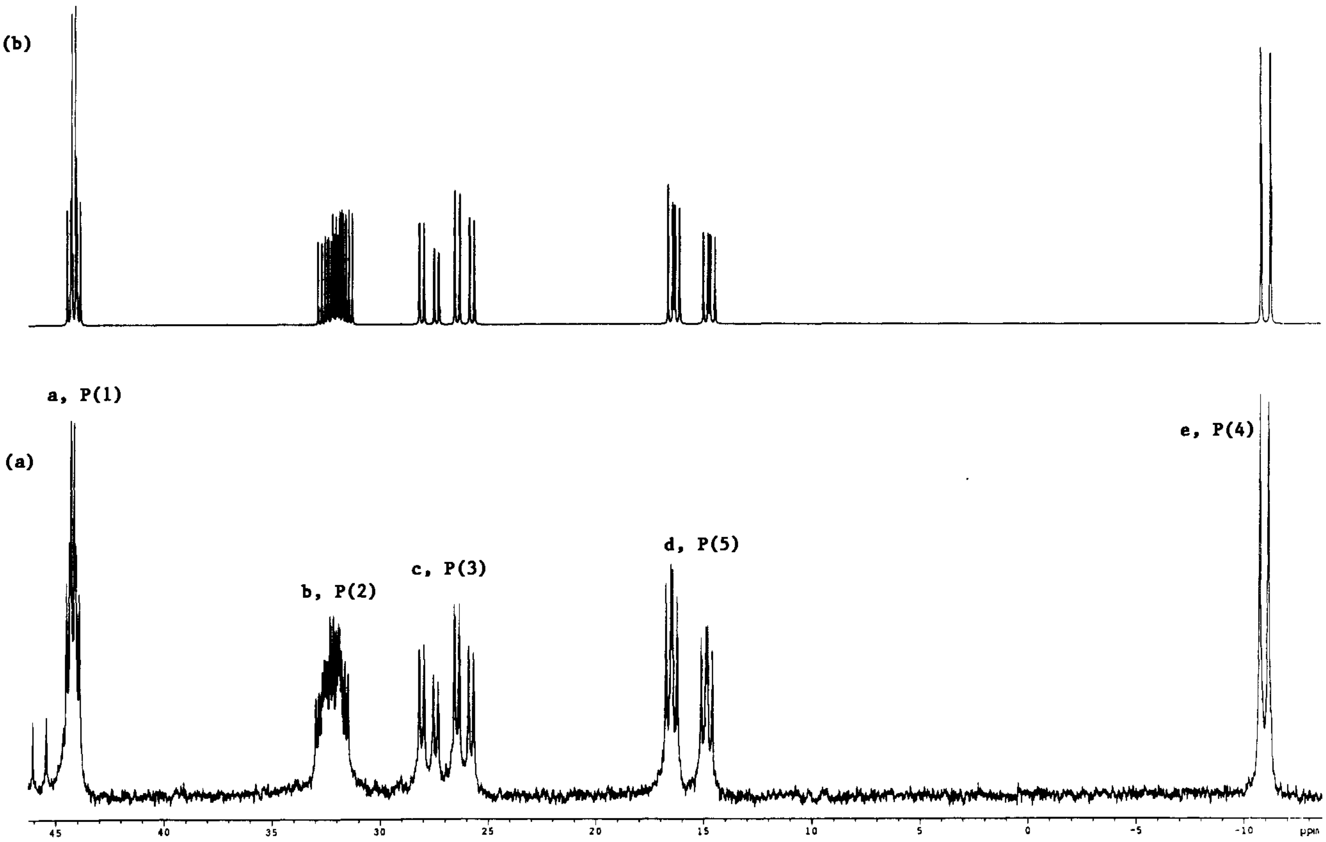

Figure 5. (a) Observed $^{31}P\{^1H\}$ NMR spectrum of *rac*-Mo$\overset{4}{-}$MoCl$_4$(PEt$_3$)(η^3-tetraphos-2) in CD$_2$Cl$_2$/CH$_2$Cl$_2$ (1:3) at 295 K. (b) Simulation of this spectrum as an ABCDE spin system.

since the intensity of this band is approximately proportional to the square of the overlap integral. However, another possible reason, namely, the "intensity-borrowing" from the nearby LMCT transition, may also play a role here.[16]

NMR Spectroscopy. The $^{31}P\{^1H\}$ NMR spectrum of *rac*-Mo$\overset{4}{-}$MoCl$_4$(PEt$_3$)(η^3-tetraphos-2) provides a unique opportunity to study ^{31}P–^{31}P couplings, through the connecting chains between the phosphorus nuclei as well as through the metal–metal quadruple bond, in quadruply bonded dinuclear systems. Corresponding to five magnetically different nuclei, the $^{31}P\{^1H\}$ NMR spectrum of *rac*-Mo$\overset{4}{-}$MoCl$_4$(PEt$_3$)(η^3-tetraphos-2) displays five multiplets a–e with relative intensities of 1:1:1:1:1 as shown in Figure 5a, along with the simulation, Figure 5b. The assignments of the peaks are based on the observed spin–spin coupling. Since the central phosphorus atom P(2) can couple with all the other four phosphorus nuclei, either through the connecting chain between P atoms or through the metal–metal bond, it will have the most complicated splitting pattern as observed for peak b centered at δ_b 39.24 ppm. In contrast, atom P(4) in the dangling unit may couple only with the central atom P(2), so it is assigned to the doublet e at δ_e −10.96 ppm. Since the coupling between the trans phosphorus atoms on the same metal center will give the largest J_{P-P} coupling constant in this system, peaks c and d, which are both doublets of quartets centered at δ_c 26.93 ppm and δ_d 15.67 ppm, respectively, are assigned to P(3) and P(5) ($^2J_{P(3)-P(5)} = 131$ Hz). The distinction between these two P atoms is based on the following difference. P(3) can couple with P(2) through both the connecting chain and the metal–metal bond, but P(5) can couple with P(2) only through the metal–metal bond. Thus the former may give a larger coupling constant, $^3J_{P(2)-P(3)} = 53$ Hz, than the later, $^3J_{P(2)-P(5)} = 24$ Hz. The remaining peak a, which is actually also a doublet of doublets of doublets centered at δ_a 44.28 ppm, is assigned to P(1). Spectrum simulation was done for an ABCDE spin system by employing the J_{P-P} coupling constants listed in Table V, and produced the result shown in Figure 5b. Previously, we have studied the $^{31}P\{^1H\}$ NMR spectra for a series of Mo$_2$X$_4$P$_4$ compounds with different bidentate phosphine ligands. Only a singlet can be obtained for compounds with ligands such as dppm, dppee, and dppe[17] since all four phosphorus nuclei are equivalent. One compound with the asymmetric phosphine dmdppm[18] displays a more complex spectrum which shows two multiplets with large J_{P-P} coupling centered at δ 17.17 and −3.26 ppm due to the AA′BB′ pattern in this system. However, no previous compound ever provided such an informative spectrum as we report here.

Table V. $^{31}P\{^1H\}$ NMR Data for *rac*-Mo$\overset{4}{-}$MoCl$_4$(PEt$_3$)(η^3-tetraphos-2)

		J_{P-P}		
nuclear	δ, ppm	coupling	exptl value, Hz	simulation, Hz
P(1)	44.28	P(1)–P(2)	12	13.55
P(2)	39.24	P(1)–P(3)	18	18.44
P(3)	26.93	P(1)–P(5)	18	18.05
P(4)	−10.96	P(2)–P(3)	53	54.92
P(5)	15.67	P(2)–P(5)	24	25.21
		P(2)–P(4)	33	35.20
		P(3)–P(5)	131	132.18

The ^1H NMR spectrum of *rac*-Mo$\overset{4}{-}$MoCl$_4$(PEt$_3$)(η^3-tetraphos-2) is shown in Figure 6. Partial assignment of this spectrum can be made as follows. The doublet of triplets centered at δ 0.596 ppm is assigned to the –CH$_3$ groups in the coordinated PEt$_3$ unit. The spin-spin coupling constants, namely, $J_{P(5)-H}$ and

---

[16] Hopkins, M. D.; Gray, H. B.; Miskowski, V. M. *Polyhedron* **1987**, *6*, 705.

[17] (a) Cotton, F. A.; Eglin, J. L.; Hong, B.; James, C. A. *J. Am. Chem. Soc.* **1992**, *114*, 4915. (b) Cotton, F. A.; Eglin, J. L.; Hong, B.; James, C. A. *Inorg. Chem.*, in press.

[18] Cotton, F. A.; Eglin, J. L.; James, C. A. *Inorg. Chim. Acta.*, in press.

[19] Chen, J.-D.; Cotton, F. A. *Inorg. Chem.* **1991**, *30*, 6.

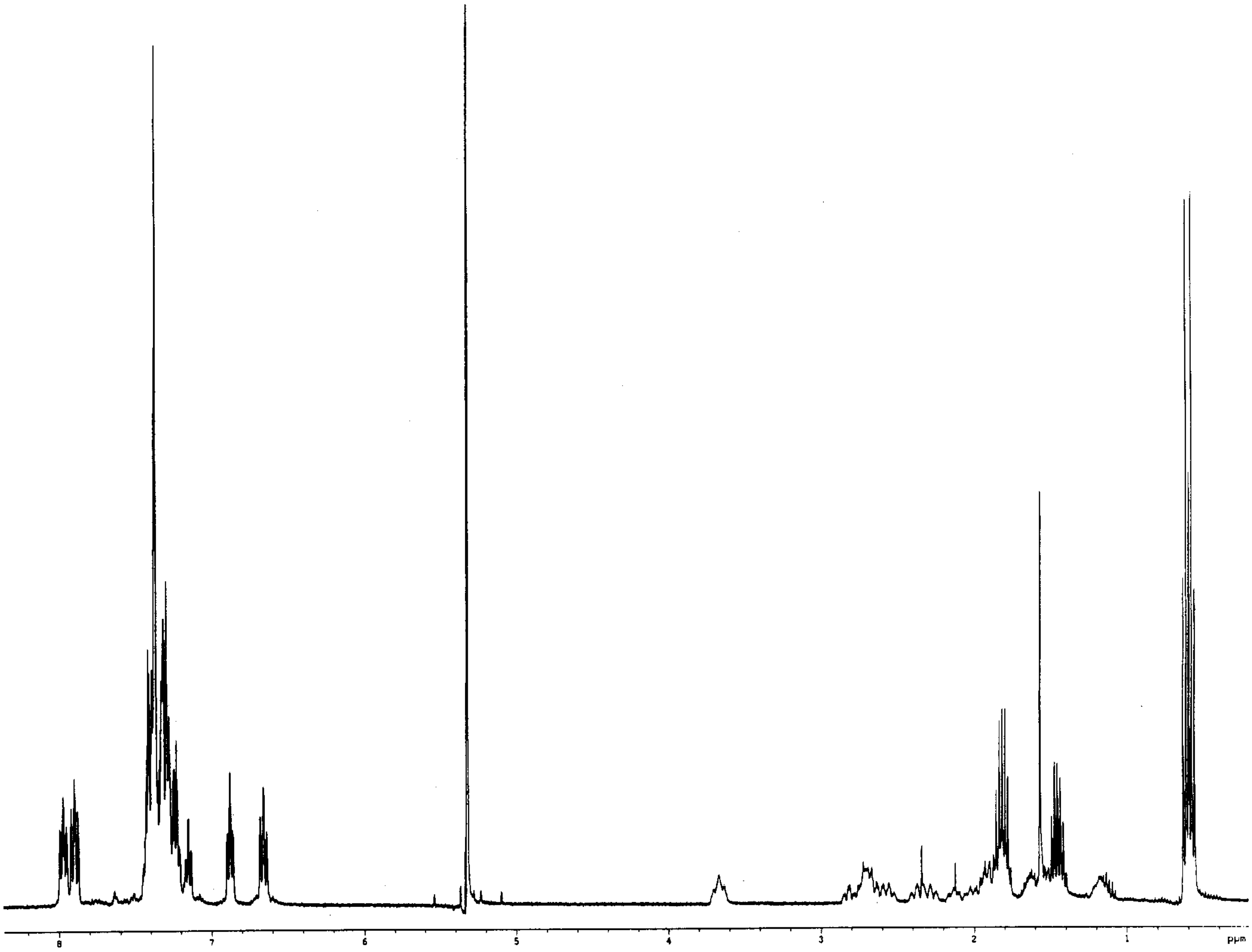

Figure 6. ^{1}H NMR spectrum of *rac*-Mo$\overset{4}{-}$MoCl$_4$(PEt$_3$)(η^3-tetraphos-2) in CD$_2$Cl$_2$ at 295 K.

J_{H-H}, in this PEt$_3$ unit are 14.4 and 7.6 Hz, respectively. The doublet of doublets of quartets centered at δ 1.636 ppm is ascribed to the –CH$_2$ group in PEt$_3$ unit. The coupling between P(5) and the two equivalent protons in this –CH$_2$ group is large, namely, 145.6 Hz. These two protons can also couple with P(3) which is trans to P(5), and this affords a $J_{P(3)-H}$ coupling constant of 22.8 Hz. The protons in the phenyl groups as well as the methylene groups on the connecting chains between phosphorus donor atoms can be assigned to peaks in the regions 6.6–8.0 and 1.1–2.9 ppm, respectively, but detailed assignment of these protons would be difficult due to the complexity of the spectrum. For the same reason it is not possible to make any quantitative assessment of the diamagnetic anisotropy of the Mo$\overset{4}{-}$Mo bond in this system.

Acknowledgment. Financial support from the National Science Foundation is gratefully acknowledged.

Supplementary Material Available: Full lists of crystallographic data, bond distances, bond angles, torsion angles, and anisotropic thermal parameters (8 pages). Ordering information is given on any current masthead page.